High-Speed Optical FSK Modulator for Optical Packet Labeling

Tetsuya Kawanishi, Kaoru Higuma, Takahisa Fujita, Junichiro Ichikawa, Takahide Sakamoto, *Member, IEEE,* Satoshi Shinada, *Member, IEEE*, and Masayuki Izutsu, *Fellow, IEEE*

***Abstract*–We described a novel optical label swapping (OLS) technique for optical packet systems using frequency-shift-keying (FSK) optical labeling. High-speed optical FSK signal can be generated by using an external FSK modulator consisting of four optical phase modulators. The FSK modulator was based on optical single-sideband (SSB) modulation technique, and comprised of traveling-wave electrodes for high-speed frequency switching. We demonstrate 10 Gbps FSK transmission, and simultaneous modulation by FSK and intensity modulation (IM). OLS using double-sideband modulation was also demonstrated, where this technique can be used for a bundled wavelength-domain-multiplexing (WDM) channels without using an array of pumping light sources.**

***Index Terms*–Frequency-shift-keying, label swap, optical modulator, optical packet.**

I. Introduction

A combination of intensity modulation (IM) and frequency shift keying (FSK) is a promising technique for optical label switching in optical packet systems [1], [2]. In this technique. payload signals are in IM format. while label information is written by FSK signal. The merit of this FSK labeling is that an FSK transmitter generates the label information on the optical canicr frequency without affecting its intensity. Simultaneously modulated IM and FSK signals are independently demodulated by using an optical filter, so that the label information can be extract without affecting the payload signal. For this purpose, fast and wideband external FSK modulation technique is required, which has never developed. In previous works, FSK signal was generated by direct modulation of electric current in a laser light source [3], [4]. Thus, FSK bit rate is limited by the response of the laser [5], [6]. Parasitic intensity modulation in the direct modulation should be compensated by using an additional intensity modulator.

Recently, however, we reported wavelength conversion by using an optical single-sideband (SSB) modulator consisting of four optical phase modulators [7], [8]. The output optical frequency depends on RF-signal frequency and dc-bias voltage fed to the modulator, which can be electronically controlled. In this paper, we investigate an optical FSK modulator based on the SSB modulator, and demonstrate high-speed FSK transmission [9], [10]. By using this modulator, we can generate IM/FSK signal with a simple setup. Moreover, we also demonstrate a novel optical FSK label swapping technique having no pumping light sources, which can be also used for WDM signals. Optical label swapping (OLS) is a promising technique for implementing packet routing and forwarding functions over optical packet networks. Previously reported OLS systems used cross modulations between optical spectral components, such as cross-phase modulation in an optical amplifier, to generate a new label signal. Thus, the OLS system should have additional light sources for the cross modulation. In an OLS system having wavelength-domain-multiplexing (WDM) channels, we have to use a pumping light source and a cross modulation device for each WDM channel, so that the setup for the OLS with WDM becomes extremely complicated.

This paper is organized as follows. In Section II, the principle of optical SSB modulation is described briefly. In Section III, by using an optical network simulator, we investigate optical frequency (wavelength) shift in WDM systems. We can shift bundled WDM channels simultaneously by an optical SSB modulator. The performance and structure of the FSK modulator are described in Section IV. High-speed optical FSK transmission was demonstrated where the FSK signal was demodulated by using an optical filter. Section V gives the principle of OLS using double-double sideband modulation. We experimentally demonstrated IM/FSK simultaneous modulation where bit rates of IM and FSK are, respectively, 10 and 1 Gbps. OLS for the IM/FSK signal was also demonstrated and pure IM channel was successfully restored by using $LiNbO_3$ (LN) Mach-Zehnder intensity modulator. Our conclusion is presented in Section VI.

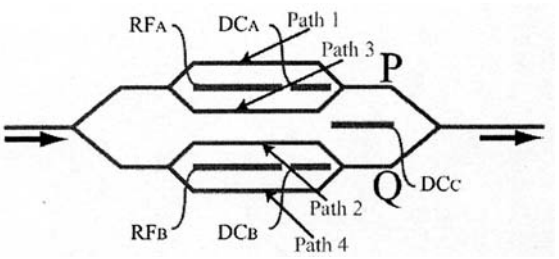

Fig. 1 . Optical SSB modutator.

II. Optical SSB Modulator

As shown in Fig. 1, the SSB modulator consists of parallel four optical phase modulators [7], [8]. The electric field of the output can be expressed by

$$E = \frac{e^{2\pi i f_0 t}}{4} \sum_{j=1}^{4} \sum_{n=-\infty}^{\infty} J_n\left(A_j^{\mathrm{RF}}\right) e^{in\left(2\pi f_m t + \phi_j^{\mathrm{RF}}\right)} \times A_j^{\mathrm{LW}} e^{i\phi_j^{\mathrm{LW}}} \quad (1)$$

Manuscript received May 28, 2004.

T. Kawanishi, T. Sakamoto, S. Shinada, and M. Izutsu are with the National Institute of Information and Communications Technology, Koganei, Tokyo 184-8795, Japan (e-mail: kawanish@nict.go.jp).

K. Higuma, T. Fujita, and J. Ichikawa are with the Sumitomo Osaka Cement, Funabashi, Chiba 274-8601, Japan.

Digital Object Identifier 10.1109/JLT.2004.840353

$$= \frac{e^{2\pi i f_0 t}}{4} \sum_{n=-\infty}^{\infty} e^{2\pi i n f_m t} \sum_{j=1}^{4} J_n\left(A_j^{\mathrm{RF}}\right) P_{n,j} A_j^{\mathrm{LW}} \quad (2)$$

where

$$P_{n,j} \equiv \exp i\left[(T - Sn) j\frac{\pi}{2} + \Delta\phi_j^{\mathrm{LW}} + n\Delta\phi_j^{\mathrm{RF}}\right] \quad (3)$$

$$\phi_j^{\mathrm{LW}} = T\frac{j\pi}{2} + \Delta\phi_j^{\mathrm{LW}} \quad (4)$$

$$\phi_j^{\mathrm{RF}} = -S\frac{j\pi}{2} + \Delta\phi_j^{\mathrm{RF}} \quad (5)$$

$$S = \pm 1, \quad T = \pm 1. \quad (6)$$

J_n expresses the first kind nth-order Bessel's function. ϕ_j^{RF} and ϕ_j^{LW} denote the phases of RF-signal and lightwave in Path j. $\Delta\phi_j^{\mathrm{RF}}$ and $\Delta\phi_j^{\mathrm{LW}}$ are the deviations of the phases from the ideal condition for the SSB modulation. A_j^{RF} is the induced optical phase due to the RF-signal in Path j , and is proportional to the amplitude of the RF-signal applied to the electrode. A_j^{LW} denotes the amplitude of lightwave in Path j . f_0 and f_{m} are the frequencies of input lightwave and RF-signal, respectively. When $\Delta_j^{\mathrm{RF}} = \Delta_j^{\mathrm{LW}} = 0$, the phases are 0, $\pi/2$, π, and $3\pi/2$ (0, 90, 180, and 270°). The SSB modulator has a pair of Mach-Zehnder structures on an x-cut LN substrate, so that we can apply RF-signals of 0, 90, 180, and 270° by feeding a pair of RF-signals with 90° phase difference at two RF-ports (RF_A, RF_B) [8]. The optical phase differences are also set to be 90°, by using dc-bias ports (dc_{A} , dc_{A} , dc_{A}). The output optical spectrum defined by (2) can be expressed by

$$E = A^{\mathrm{LW}} e^{2\pi i f_0 t} \sum_{n=0}^{\infty} J_N(A^{\mathrm{RF}}) e^{2\pi i N f_m t} \quad (7)$$

$$= A^{\mathrm{LW}} U e^{2\pi i f_0 t} \times \left[J_1(A^{\mathrm{RF}}) e^{2\pi i U f_m t} - J_3(A^{\mathrm{RF}}) e^{-3\cdot 2\pi i U f_m t} + J_5(A^{\mathrm{RF}}) e^{5\cdot 2\pi i U f_m t} - J_7(A^{\mathrm{RF}}) e^{-7\cdot 2\pi i U f_m t} + \cdots\right] \quad (8)$$

where N and U are defined by

$$N \equiv U \times (2n+1) \times (-1)^n \quad (9)$$

$$U \equiv S \times T. \quad (10)$$

When the intensity of the electric field is so small that we can neglect high-order harmonic generation at the optical phase modulation, the output for $U = 1$ can be approximately expressed by

$$E \simeq A^{\mathrm{LW}} e^{2\pi i f_0 t}\left[J_1(A^{\mathrm{RF}}) e^{i2\pi f_m t} - J_3(A^{\mathrm{RF}}) e^{-3\cdot 2\pi i f_m t}\right]. \quad (11)$$

Because $J_1 > J_3$, the dominant component in the output is the first-order upper sideband (USB), which corresponds to the frequency shifted component, Fig. 2 shows the principle of the SSB modulation. Each sub-Mach-Zehnder structure (the pair of Path 1 and 3, or that of Path 2 and 4) is in null-bias point. Thus, the input lightwave component ($e^{2\pi i f_0 t}$) is vanished and lower and upper sidebands are generated. Due to the 90° phase differences in the RF-signal and the lightwave, the polarity of lower sideband (LSB) component at point "P" is the opposite of "Q." The LSB would be vanished at the output port, so that the SSB modulated signal consisting of USB can be obtained. On the other hand, in the case of $U = -1$, LSB can be generated instead of USB. We can easily switch the polarity of T, by changing the dc-bias voltage applied on the port dc_C. The signal-to-noise ratio (SNR) and conversion efficiency of the frequency shift by the modulator are given by $J_1(A^{\mathrm{RF}})/J_3(A^{\mathrm{RF}})$ and $J_1(A^{\mathrm{RF}})$, respectively (see Fig. 3). The conversion efficiency has a maximum of 0.582 (–5.36 dB) when the induced phase A^{RF} is equal to 1.84 rad. As shown in (8), the output lightwave has undesired high-order sideband components whose orders are –3, +5, –7, . . . for $U = +1$, and 3, –5, +7, . . . for $U = -1$. Thus, the frequency difference between the generated spectral components equals $4f_m$. We note that the dominant high-order component (J_3) can be suppressed by using a predistortion technique [11].

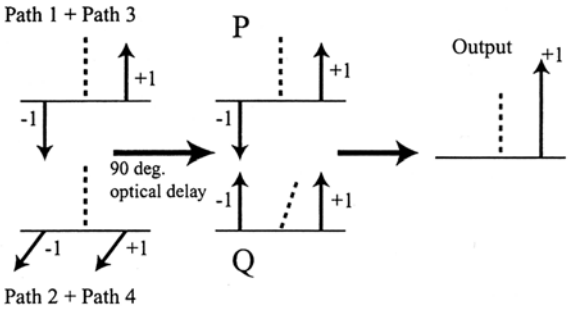

Fig. 2. Principle of optical SSB modulation.

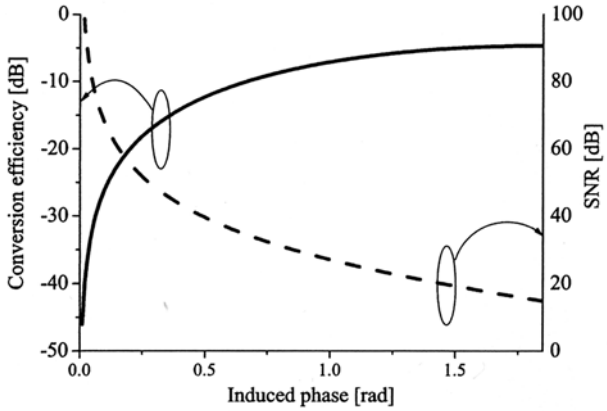

Fig. 3. Conversion efficiency and SNR ot wavelength shifter using SSB modutation.

III. Numerical Analysis of Optical Frequency Shift in WDM Systems

We investigated the optical frequency shift with the SSB modulator in WDM systems, by using a lightwave network simulator, *Optisystem*™ 2.2. As shown in Fig. 4, the WDM system has 9 channels with 25 GHz spacing. The bit rate and the optical frequency of the nth channel were, respectively, $2.5 \times [(n - 5) \times (r/100 + 1)]$ Gbps and $193.5 + (n - 5) \times 0.025$ THz, where $r = 2.0$. Thus, the bit rate of the fifth channel was 2.5 Gbps. Those of neighboring channels were 2% higher or lower than that of the fifth, to suppress unphysical crosstalks which are due to the finite time windows in this simulation. The sampling rate in the simulator was 160 Gbps, while the time window was 40.96 ns, which was limited by the memory size and the processor speed of the computer we used. The nonreturn-to-zero

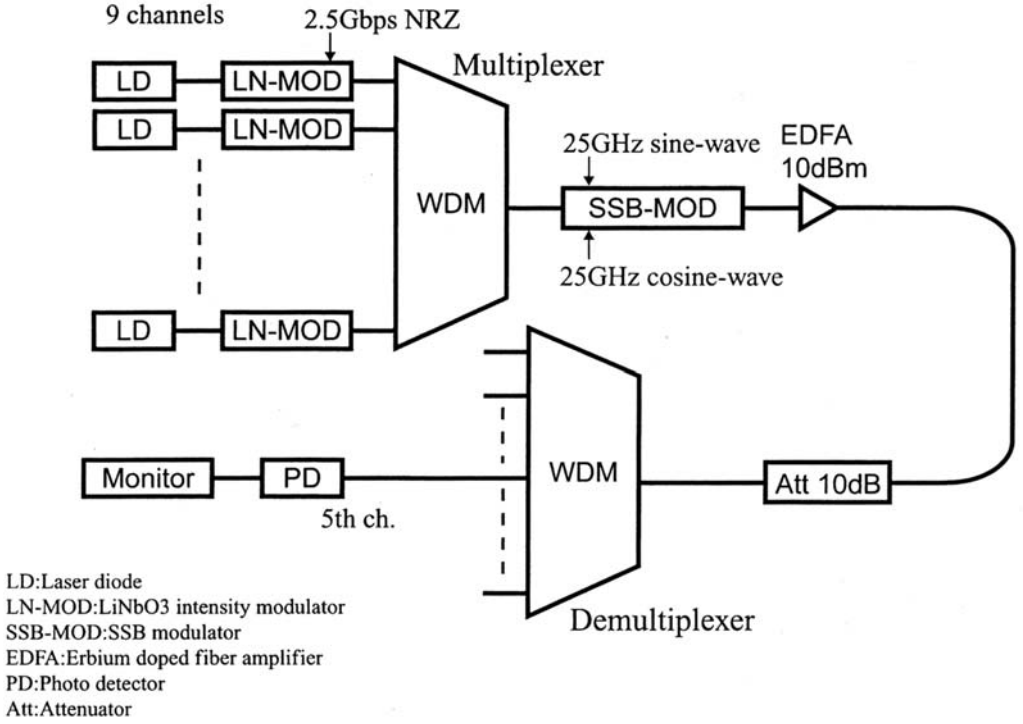

Fig. 4. Model for a 2.5-Gbps WDM system with a wavelength shifter using SSB modulation.

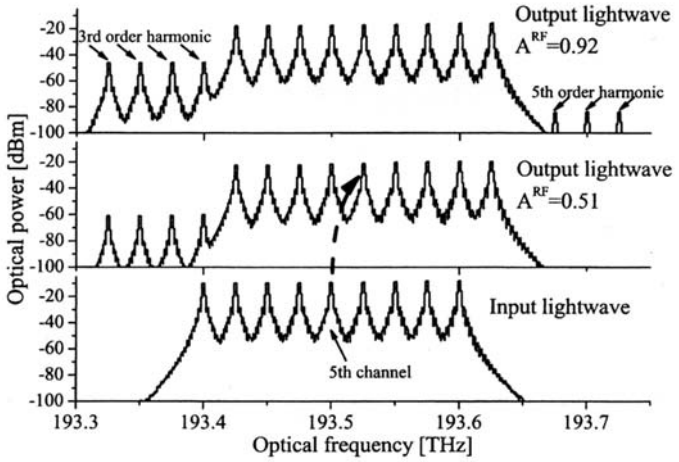

Fig, 5. Input and output opticat spectra of the SSB modutator.

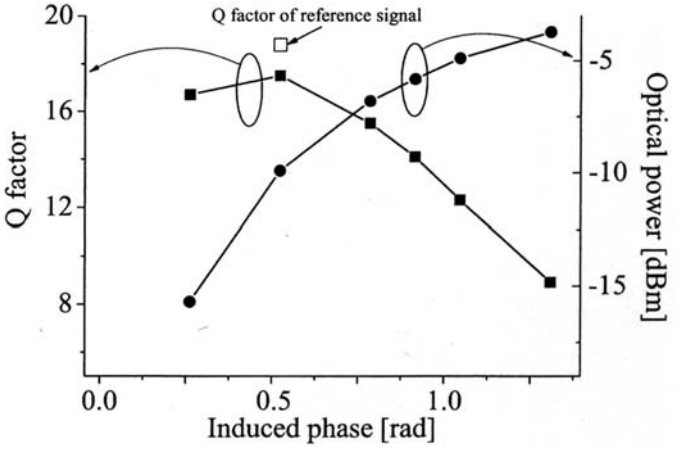

Fig. 6. Q-factor ot the firth channel measured by an electric signal monitor, and the total optical power at the output port of the SSB modulator, Q-factor of the reference signal was 18.8, where an attenuator was placed at the output port of the WDM muttiplexer instead ot the SSB modutator.

(NRZ) signals were generated by LN optical intensity modulators. We used a model for the SSB modulator consisting of four optical phase modulators as shown in Fig. 1. The lightwave signals were fed to the SSB modulator via a WDM multiplexer. To compensate the loss at the wavelength shift, an EDFA was put at the output lightwave port of the modulator, where the output power was controlled to be 10 dBm by tuning the pump laser power. The noise figure of the EDFA was assumed to be 4 dB . We calculated the optical spectra at the input and the output port of the SSB modulator with the resolution of 0.01 nm. As shown in Fig. 5, optical frequency shift (25 GHz) of WDM channels was successfully demonstrated in this simulation. The undesired third-order sideband components were also generated in the output spectra. The frequency difference between the desired frequency shifted component (the first-order USB) and the undesired sideband was $4f_m$, so that there were four peaks of them in the spectrum. The other third-order components were overlapped with the desired components. In the case of $A^{RF} = 0.92$, the fifth-order sidebands were also generated, in addition to the third-order sidebands which were dominant in undesired components. Fig. 6 shows Q-factors of the fifth channel at the electric signal monitor in Fig. 4, and the total optical power at the output port of the SSB modulator. The electric output of the photodetector was fed to the monitor via a transimpedance amplifier whose impedance was 600 Ω and noise figure was 6 dB. Q-factor of the reference signal. where an attenuator was placed at the output port of the WDM multiplexer instead of the SSB modulator, was also shown in Fig. 6. The output power was an increasing function of the induced phase A^{RF}. However, the SNR of the output signal was an decreasing

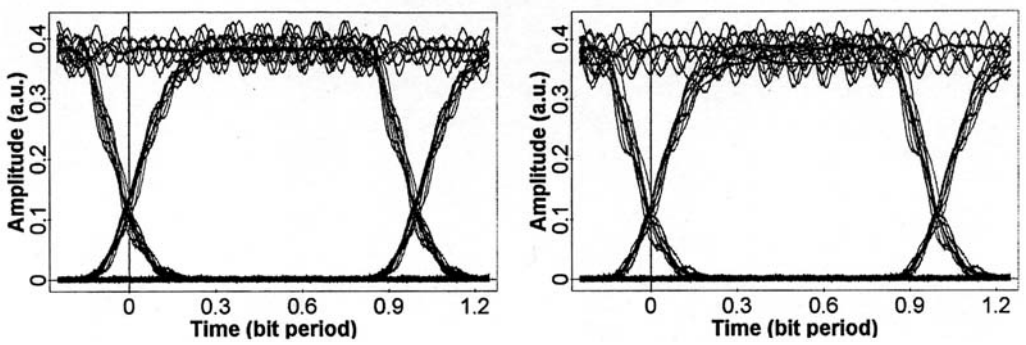

Fig. 7. Eye-diagrams of the reference signal (right) and the frequency-shifted fifth channel (left), where induced phase was 0.46 rad.

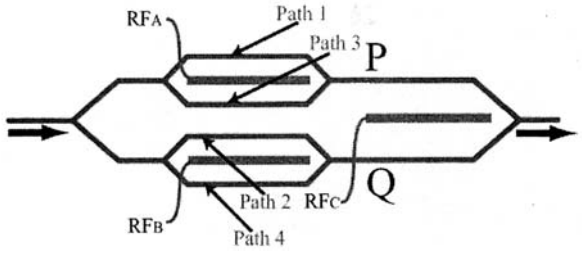

Fig. 8. Optical FSK modulator.

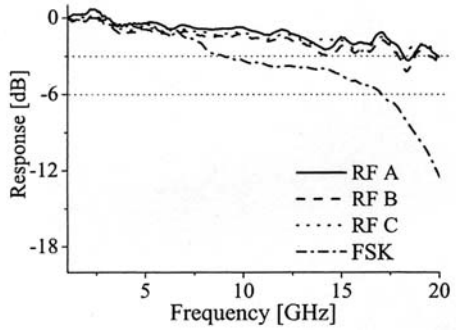

Fig. 9. Frequency response of FSK modulator.

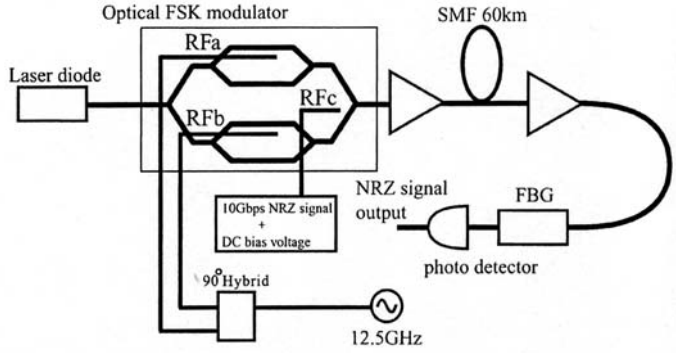

Fig. 10. Setup for FSK transmission.

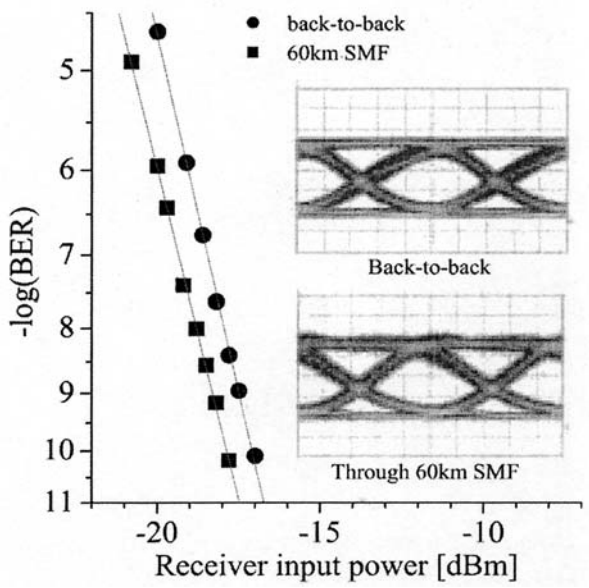

Fig. 11. Bit-error-ratio curves and eye-diagrams of 9.95 Gbps FSK.

function as shown in Fig. 3. Due to this tradeoff relations, the Q-factor had a peak around $A^{RF} = 0.5$. Fig. 7 shows the eye-diagrams of the reference signal and the fifth channel. In the frequency shifted signal, the deviation of the mark level was larger than that of the reference. We deduce that this is due to interference between the desired channel and the high-order harmonic components of the other WDM channels.

IV. FSK Modulator

The FSK modulator consists of parallel four optical phase modulators as shown in Fig. 8. The device structure is almost the same in the SSB modulator, but the FSK modulator has an electrode (RF_C) for high-speed FSK signal, instead of an dc-bias electrode (dc_C) in the SSB modulator. When we apply a pair of RF-signals, which are of the same frequency f_m and have a 90° phase difference, to the electrodes RF_A and RF_B, frequency shifted lightwave can be generated at the output port of the modulator. A sub-Mach-Zehnder structure of path 1 and 3 should be in null-bias point (lightwave signals in the paths have 180° phase difference), where the dc-bias can be controlled by RF_A . The other sub-Mach-Zehnder structure of path 2 and 4 are also set to be in null-bias point by using RF_B. To eliminate USB or LSB, the lightwave signal in each path also should have 90° phase difference each other, as described in Section II. When the phase difference induced by RF_C is ±90° , we can get carrier-suppressed single sideband modulation comprising one of the sideband components (USB or LSB). Thus, the optical frequency of output lightwave can be switched by changing the induced phase at RF_C. In the SSB modulator, the electrode for optical phase control dc_C was not designed for high-speed operation, so that the switching time was limited by the response of the electrode. On the other hand, the FSK modulator has the electrode RFC for high-speed optical phase switch at the junction of a pair of sub-Mach-Zehnder structures. The amplitudes of USB and LSB are, respectively, described by

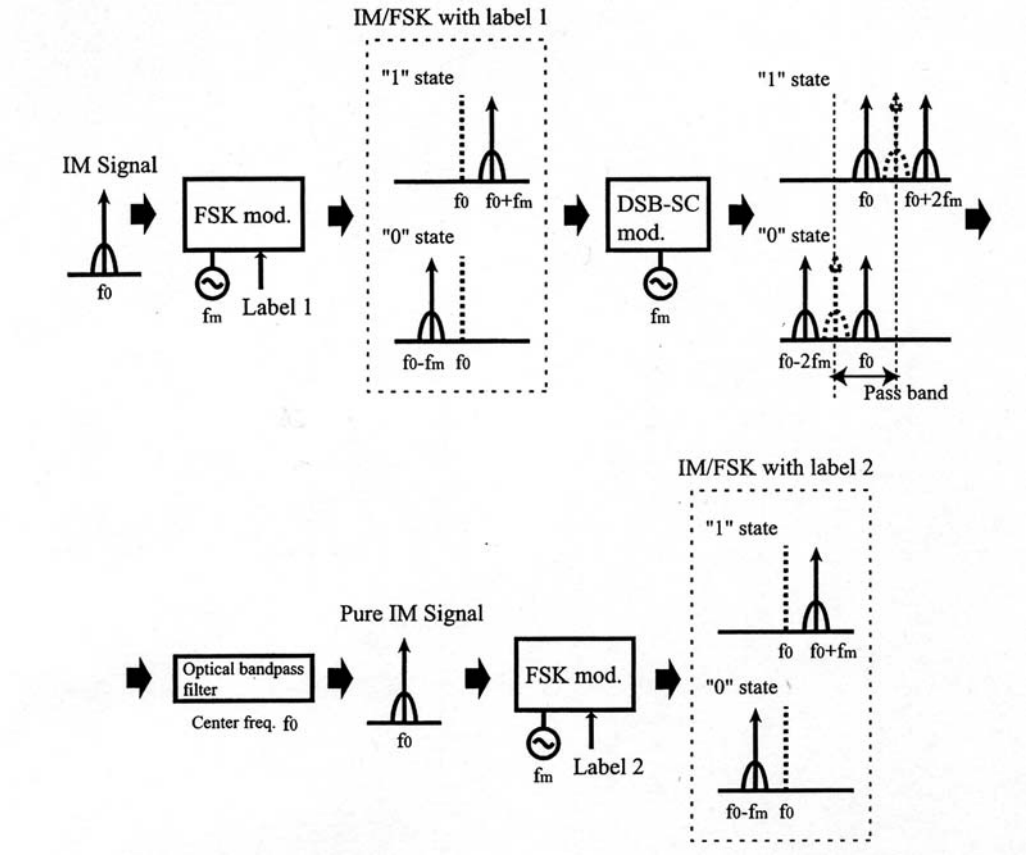

Fig. 12. Principle of OLS of IM/FSK signal.

$[1 + i \exp(i\phi_{FSK})]/2$ and $[-1 + i \exp(i\phi_{FSK})]/2$, where ϕ_{FSK} is the induced phase difference at RF_C, and $\phi_{FSK} = -90^\circ$ corresponds to an optimal condition for USB generation ($U = 1$) . Thus, by feeding an NRZ signal, whose zero and mark levels correspond to $\phi_{FSK} = -90, +90^\circ$, to RF_C, we can generate an optical FSK signal, without any parasitic intensity modulation. The bandwidth for the FSK signal should be smaller than the RF-frequency f_m , when the FSK signal is demodulated by optical filters.

We fabricated an optical FSK modulator having a $LiNbO_3$ lightwave circuit with traveling wave electrodes to obtain high-speed response. Fig. 9 shows the frequency responses of the modulating electrodes. The rise time was around 100 ps, which was limited by driver and receiver circuits, and 3 dB bandwidths of the electrodes (RF_A, RF_B, and RF_C) were around 18 GHz. Thus, the wavelength switching time of the optical FSK modulator would be less than 100 ps. We also measured the FSK response by feeding a sinusoidal signal to RF_C. The FSK signal was demodulated into an IM signal by an optical filter. As shown in Fig. 9, 6 dB bandwidth was 17 GHz, where the FSK response over 10 GHz Was diminished, because some part of the FSK signal becomes out of the passband of the optical filter, whose bandwidth was about 20 GHz. We also measured bit-error ratio (BER) performance of FSK transmission. As shown in Fig. 10, a 9.95-Gbps NRZ ($2^{31} - 1$ pseudorandom binary sequence (PRBS) signal was applied to RF_C of the FSK modulator, where a fiber Bragg grating (FBG) was used to convert an FSK signal into an IM signal for demodulation. Fig. 11 shows BER curves and eye-diagrams of 9.95 Gbps FSK for back-to-back, and after transmission through a 60-km single-mode fiber (SMF). The RF frequency f_m was 12.5 GHz. The results show that the eyes are clearly open and that error-free transmission of 10 Gbps FSK-60 km SMF is possible. Power penalties of 60 km transmission with reference to back-to-back at – log(BER) = 9 was –0.8 dB. We deduce that the negative penalty was due to the dispersion of the FBG.

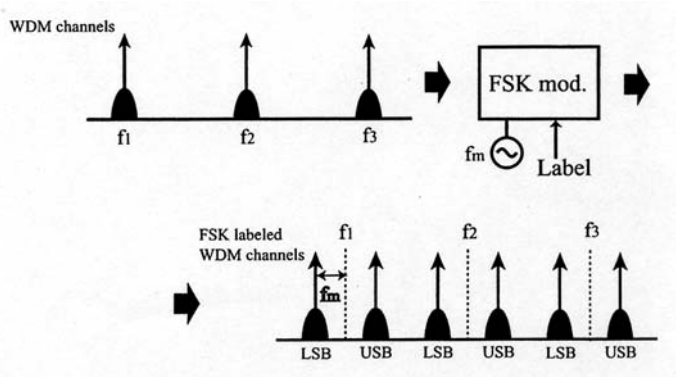

Fig. 13. FSK labeling on bundled WDM channels.

V. IM/FSK Modulation and OLS Using Double-Sideband Modulation

Fig. 12 shows the principle of OLS using double-sideband modulation technique. IM/FSK signal has a pair of optical carriers whose frequencies $f_0 - f_m$ and $f_0 + f_m$, where f_0 is the optical carrier frequency at the output port of the light source. f_m denotes the frequency of modulating signal fed to the electric

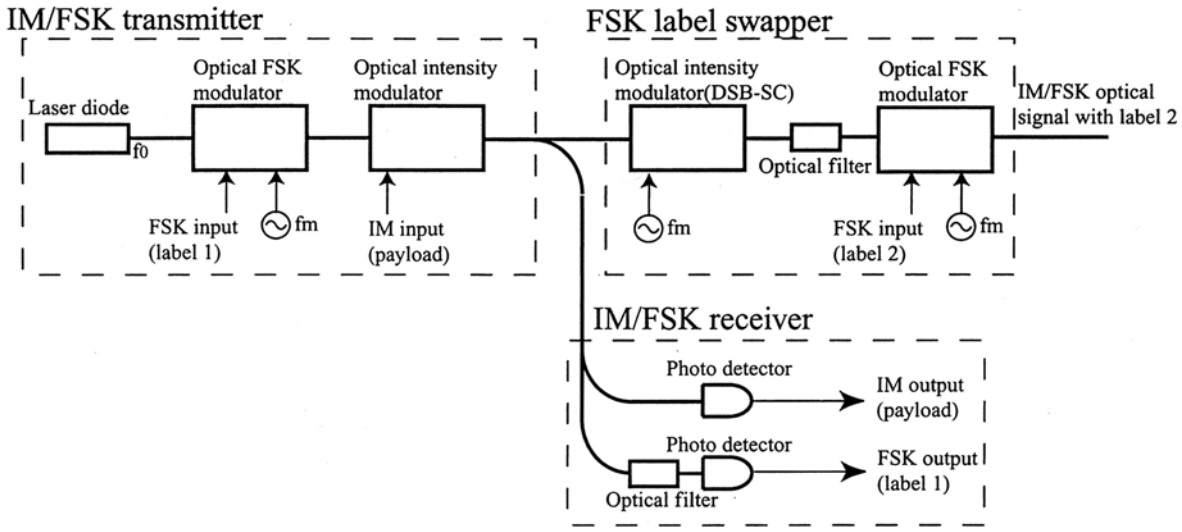

Fig. 14. Setup and experimental results of IM/FSK modulation and OLS using DSB-SC.

input ports RF_A and RF_B of the FSK modulator. When the FSK switching signal fed to RF_C is in "1" state where the modulator generates USB ($\phi_{FSK} = -90^\circ$), the output carrier frequency is $f_0 + f_m$. That of "0" state, where the modulator generates LSB ($\phi_{FSK} = +90^\circ$), is $f_0 - f_m$. The IM/FSK signal is fed to an intensity modulator which is in null-bias point to obtain double-sideband suppressed carrier (DSB-SC) modulation. The modulating signal is a sinusoidal wave whose frequency is f_m. The output has three optical spectral components whose carriers are $f_0 - 2 f_m$, f_m and $f_0 + 2 f_m$. When the FSK switching signal is in "1" state, the output of the intensity modulator has two carriers of f_0 and $f_0 + 2f_m$. On the other hand, the output of "0" has two carriers of f_0 and $f_0 - 2 f_m$. The output always has the f_0 component regardless of the FSK switching signal. Thus, by using an optical bandpass filter whose center frequency is f_0, we can remove the FSK signal from the IM/FSK signal, and restore a pure IM signal which does not have an FSK signal. The output of the DSB-SC modulation has only one optical carrier of f_0 , so that we can add a new FSK label by using another FSK modulator.

As shown in Fig. 13, the FSK modulator can be used for a WDM signal which has many IM channels. We can simultaneously shift the carrier frequencies of the channels by one FSK modulator, as described in Section III. For an FSK-WDM signal, an optical filter which has a periodic optical frequency response, such as an interleaver, an arrayed-waveguide, and so on, can be used to demodulate the FSK signal. The proposed label swapping technique is also applicable to WDM systems by using an optical filter having the periodic response.

The setup for IM/FSK modulation and our proposed OLS system is shown in Fig. 14. We experimentally demonstrated simultaneous transmission of IM (9.95 Gbps) and FSK (1 Gbps), which are NRZ PRBS ($2^{31} - 1$) signals. The frequency deviation of FSK (f_m) was 12.5 GHz. The extinction ratio of the IM modulation was 3.9 dB. Residual IM in the FSK modulation was so small that the IM output which can be generated just by feeding the IM/FSK signal to a high-speed photodetector has a clearly opened eye-diagram. The FSK signal was demodulated by using an optical filter which can discriminate between USB and LSB.

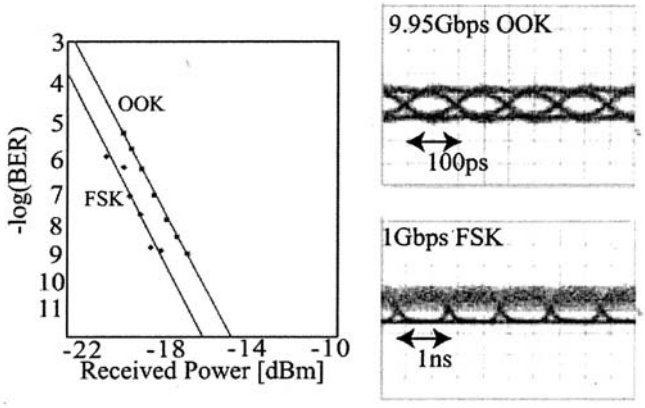

Fig. 15. BER curves and eye-diagrams for FSK and IM signals.

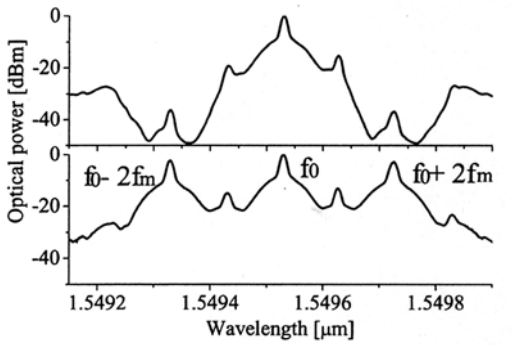

Fig. 16. Opticat spectra at the output port ot the DSB modulator (tower) and at the output port ot the optical bandpass filter (upper).

Fig. 15 shows BER curves and eye-diagrams of the FSK and IM signals, where error-free transmissions for FSK and IM were obtained. By using DSB-SC modulation, we demonstrated the restoration of a pure IM signal which has one optical carrier. Fig. 16 shows the optical spectra at the output port of the DSB modulator and at the output port of the optical bandpass filter. The spectral components of $f_0 - 2 f_m$, f_0 and $f_0 + 2 f_m$ were generated at the DSB modulator. The restored pure IM signal having the fo compopent was extracted by the bandpass filter. We also

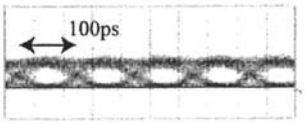

Fig. 17. Eye-diagram of restored pure OOK signal at the output port of the optical bandpass filter.

obtained clear eye-opening and error-free transmissions for the restored IM, as shown in Fig. 17. An IM/FSK signal with a new FSK label can be generated by another FSK modulator placed at output port of the optical filter, so that we can construct a simple OLS system consisting of a DSB-SC and an FSK modulators.

VI. Conclusion

In summary, by using an optical modulator consisting of four phase modulators, we have demonstrated FSK transmission with a record high bit rate of 10 Gbps. IM/FSK modulation was also demonstrated, where we can get error-free transmission for the payload in 10 Gbps IM and the label in 1 Gbps FSK. In addition, we proposed a novel label swapping technique without using optical cross modulation, which can be also applicable to WDM systems by one DSB-SC modulator.

References

[1] J. J. V. Olmos, I. T. Monroy, and A. M. J. Koon, "High bit-rate combined FSK/IM modulated optical signal generation by using GCSR tunable laser sources," *Opt. Expr*, vol. 11 , pp. 3136–3140, 2003.

[2] K. Vlachos, J. Zhang, J. Cheyns, Sulur, N. Chi, E. Van Breusegem, I. T. Monroy, J. G. L. Jennen, P. V. Holm-Nielsen, C. Peucheret, R. O'Dowd, P. Demeester, and A. M. J. Koonen, "An optical IM/FSK coding technique for the implementation of a label-controlled arrayed waveguide packet router," *J. Lightw. Technol*., vol. 21 , pp. 2617–2628, 2004.

[3] Y. Yu, G. Mulvihill, S. O'Duill, and R. O'Dowd, "Performance implications of wide-band lasers for FSK modulation labeling scheme," *IEEE Photon. Technol. Lett*., vol. 16, pp. 39–41, 2004.

[4] J. Zhang, N.Chi, P. V. Holm-Nielsen,C. Peucheret, and P. Jeppesen,"An optical FSK transmitter based on an integrated DBF laser-EA modulator and its application in optical labeling," *IEEE Photon. Technol. Lett*., vol. 15, pp. 984–986, 2003.

[5] K. Iwashita, T. Imai, T. Matsumoto, and G. Motosugi, "400 Mbits optical FSK transmission experiment over 270 km of single-mode fiber," *Electron. Lett*., vol. 22, pp. 161–165, 1986

[6] R. S. Vodhanel, J L. Gimlett, N. K. Cheung, and S. Tsuji, "FSK heterodyne transmission experiments at 560 Mbit/s and 1 Gbit/s," *J. Lightw. Technol*., vol 5, pp. 461–468, 1987.

[7] S. Shimotsu, S. Oikawa, T. Saitou, N. Mitsugi, K. Kubodera, T. Kawanishi, and M. Izutsu, "Single side-band modulation performance of a $LiNbO_3$ integrated modulator consisting of four-phase modulator waveguides," *IEEE Photon. Technol. Lett*., vol. 13, pp. 364–366, 2001 .

[8] K. Higuma, S. Oikawa, Y. Hashimoto, H. Nagata, and M. Izutsu, "X-cut lithium niobate optical single-sideband modulator," *Electron. Lett*., vol. 37, pp. 515–516, 2001.

[9] T. Kawanishi, K. Higuma, T. Fujita, J. Ichikawa, S Shinada, T. Sakamoto, and M. Izutsu, "Optical FSK/IM signal generation using an integrated optical FSK modulator," *IEICE Electron. Express*, vol. 1 , pp. 69–72, 2004.

[10] T. Kawanishi, K. Higuma, T. Fujita, J. Ichikawa, T. Sakamoto, S. Shinada, and M. Izutsu, "High-speed $LiNbO_3$ optical FSK modulator," Electron., Lett., to be published.

[11] T. Kawanishi and M. Izutsu, "Linear single-sideband modulation for high-SNR wavelength conversion," *IEEE Photon. Technol. Lett*. , vol. 16, pp. 1534–1536, 2004.

Tetsuya Kawanishi received the B.E., M.E., and Ph.D. degrees in electronics from Kyoto University, Kyoto, Japan, in 1992, 1994, and 1997, respectively.

From 1994 to 1995, he was with the Production Engineering Laboratory, Matsushita Electric Industrial (Panasonic) Co., Ltd. In 1997, he was with Venture Business Laboratory of Kyoto University, where he was engaged in research on electromagnetic scattering and on near-field optics. He joined the Communications Research Laboratory, Ministry of Posts and Telecommunications (now the National Institute of Information and Communications Technology), Koganei, Tokyo, in 1998. In 2004, he was a Visiting Scholar with the Department of Electrical and Computer Engineering, University of California, San Diego. He is currently a Senior Researcher with the National Institute of Information and Communications Technology, and is working on high-speed optical modulators and on RF photonics

Dr. Kawanishi received the URSI Young Scientists Award in 1999.

Kaoru Higuma received the B.E. and M.E. degrees in physics from Waseda University, Tokyo, Japan, in 1994 and 1996, respectively.

In 1996, he joined the Opto-Electronics Research Division, New Technology Research Laboratories, Sumitomo Osaka Cement Co., Ltd., Chiba, Japan. He has been engaged in the research and development of LN optical modulators.

Takahisa Fujita received the B.E. degree from the Department of Materials Technology, Chiba University, Chiba, Japan, in 2000.

In 2000, he joined the Opto-Electronics Research Division, New Technology Research Laboratories, Sumitomo Osaka Cement Co., Ltd., Chiba. He has been engaged in the research and development of optical modulators.

Junichiro Ichikawa received the B.S. and M S. degrees in mineralogy from the University of Tokyo, Tokyo, Japan, in 1987 and 1989, respectively.

In 1989, he joined the Opto-Electronics Division of Sumitomo Osaka Cement Co., Ltd., Chiba, Japan, where he has been engaged in research and development of ferroelectric material-based devices.

Takahide Sakamoto was born in Hyogo Prefecture, Japan, on May 23, 1975 He received the B.S., M.S., and Ph.D. degrees in electronic engineering from the University of Tokyo, Tokyo, Japan, in 1998, 2000, and 2003, respectively.

In 2003, he joined the Communications Research Laboratory (now National Institute of Information and Communicatlons Technology), Tokyo. He has been engaged in all-optical signal processing based on nonlinear optics. His current interest is in electrooptic devices, such as $LiNbO_3$ modulators, and their applications to photonic communication systems.

Dr. Sakamoto is a Member of the IEEE Lasers and Electro-Optics Society (LEOS) and the Institute of Electronics, Information and Communication Engineering (IEICE) of Japan.

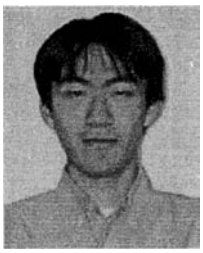

Satoshi Shinada received the B.S. degree from the Science University of Tokyo, Tokyo, Japan, in 1998 and the M.E. and Ph.D. degrees from the Tokyo Institute of Technology in 2000 and 2002, respectively.

During his Ph.D. work, he studied optical near-field generated by vertical-cavity surface-emitting lasers. In 2002, he joined the Precision and Intelligence Laboratory, Tokyo Institute of Technology, as a JSPS Postdoctoral Fellow. In 2003, he joined the National Institute of Information and Communications Technology (NICT). His current research is resonant-type $LiNbO_3$ optical modulators with antenna array.

Dr. Shinada received the IEEE/LEOS Student Award in 2002. He is a member of the Japan Society of Applied Physics and the Institute of Electronics, Information and Communication Engineers of Japan.

Masayuki Izutsu received the B.Eng., M.Eng., and D.Eng. degrees in electrical engineering from Osaka University, in 1970, 1972, and 1975, respectively.

In 1975, he joined the Department of Electrical Engineering, Faculty of Engineering Science, Osaka University, where he worked in the field of guided-wave optoelectronics. From 1983 to 1984, he was a Senior Visiting Research Fellow with the Department of Electronics and Electrical Engineering, University of Glasgow, Scotland. In 1996, he joined the Communications Research Laboratory, Ministry of Posts and Telecommunications (from April 1, 2004, National Institute of Information and Communications Technology), and is now Distinguished Researcher and Acting Leader of Integrated Photonics Group, Basic and Advanced Research Division.

Dr. Izutsu received the Paper Award and the Award For Significant Achievement in 1981 and 1988, respectively, from the Institute of Electronics, Inforrnation and Communication Engineers.